The Wide Field Imager of the International X-ray Observatory

A. Stefanescu [a,b,*], M.W. Bautz [c], D.N. Burrows [d], L. Bombelli [e,f], C. Fiorini [e,f], G. Fraser [g], K. Heinzinger [h], S. Herrmann [a,i], M. Kuster [j], T. Lauf [a,i], P. Lechner [h], G. Lutz [a,k], P. Majewski [h], A. Meuris [a,i], S.S. Murray [l], M. Porro [a,i], R. Richter [a,k], A. Santangelo [m], G. Schaller [a,i], M. Schnecke [a,k], F. Schopper [a,i], H. Soltau [h], L. Strüder [a,i], J. Treis [a,n], H. Tsunemi [o], G. de Vita [a,i], J. Wilms [p,q]

[a] Max-Planck-Institut Halbleiterlabor, Otto-Hahn-Ring 6, 81739 München, Germany
[b] Johannes Gutenberg-Universität, Inst. f. anorganische und analytische Chemie, 55099 Mainz, Germany
[c] Kavli Institute for Astrophysics and Space Research, Massachusetts Institute of Technology, Cambridge, MA 02139-4307, USA
[d] Department of Astronomy and Astrophysics, Pennsylvania State University, University Park, PA 16802, USA
[e] Politecnico di Milano, Dipartimento di Elettronica e Informazione, Milano, Italy
[f] INFN Sezione di Milano, Milano, Italy
[g] Space Research Centre, Department of Physics and Astronomy, University of Leicester, University Road, Leicester LE1 7RH, UK
[h] PNSensor GmbH, Römerstr. 28, 80803 München, Germany
[i] Max-Planck-Institut für extraterrestrische Physik, Giessenbachstr., 85748 Garching, Germany
[j] Technische Universität Darmstadt, Institut für Kernphysik, Schlossgartenstr. 9, 64289 Darmstadt, Germany
[k] Max-Planck-Institut für Physik, Föhringer Ring 6, 80805 München, Germany
[l] Harvard/Smithsonian Center for Astrophysics, 60 Garden Street, MS-67, Cambridge, MA 02138, USA
[m] Institut für Astronomie und Astrophysik, Sand 1, 72076 Tübingen, Germany
[n] Max-Planck-Institut für Sonnensystemforschung, Max-Planck-Str. 2, 37191 Katlenburg-Lindau, Germany
[o] Department of Earth and Space Science, Graduate School of Science, Osaka University, Toyonaka, Osaka 560-0043, Japan
[p] Dr. Karl Remeis-Sternwarte, Astronom. Inst. d. Univ. Erlangen-Nürnberg, Sternwartstr. 7, 96049 Bamberg, Germany
[q] Erlangen Center for Astroparticle Physics (ECAP), Erwin-Rommel-Str. 1, 91058 Erlangen, Germany

ARTICLE INFO

ABSTRACT

The International X-ray Observatory (IXO) will be a joint X-ray observatory mission by ESA, NASA and JAXA. It will have a large effective area ($3\,m^2$ at 1.25 keV) grazing incidence mirror system with good angular resolution (5 arcsec at 0.1–10 keV) and will feature a comprehensive suite of scientific instruments: an X-ray Microcalorimeter Spectrometer, a High Time Resolution Spectrometer, an X-ray Polarimeter, an X-ray Grating Spectrometer, a Hard X-ray Imager and a Wide-Field Imager.

The Wide Field Imager (WFI) has a field-of-view of 18 ft × 18 ft. It will be sensitive between 0.1 and 15 keV, offer the full angular resolution of the mirrors and good energy resolution. The WFI will be implemented as a 6 in. wafer-scale monolithical array of 1024×1024 pixels of $100 \times 100\,\mu m^2$ size. The DEpleted P-channel Field-Effect Transistors (DEPFET) forming the individual pixels are devices combining the functionalities of both detector and amplifier. Signal electrons are collected in a potential well below the transistor's gate, modulating the transistor current. Even when the device is powered off, the signal charge is collected and kept in the potential well below the gate until it is explicitly cleared. This makes flexible and fast readout modes possible.

© 2010 Elsevier B.V. All rights reserved.

1. The IXO mission

The International X-ray Observatory (IXO) is a joint effort by NASA, ESA and JAXA to build the next-generation observatory-class X-ray mission.

Fig. 1 shows a conceptual view of the IXO spacecraft and instrument platform as proposed in a NASA study. Its key component is a grazing incidence angle X-ray mirror system with more than $A_{eff} = 3\,m^2$ (at 1.25 keV) effective area, $f = 20\,m$ focal length and 5 in. angular resolution.

As observatory facility, IXO will provide new insights into a broad range of astrophysical questions. For the Astro2010 Decadal Survey, a large number of white-papers were submitted that showcase the diverse science IXO is going to perform. Three overarching topics can be highlighted: *matter under extreme conditions* (e.g. Refs. [1–3]), *formation of structure* (e.g. Refs. [4–6])
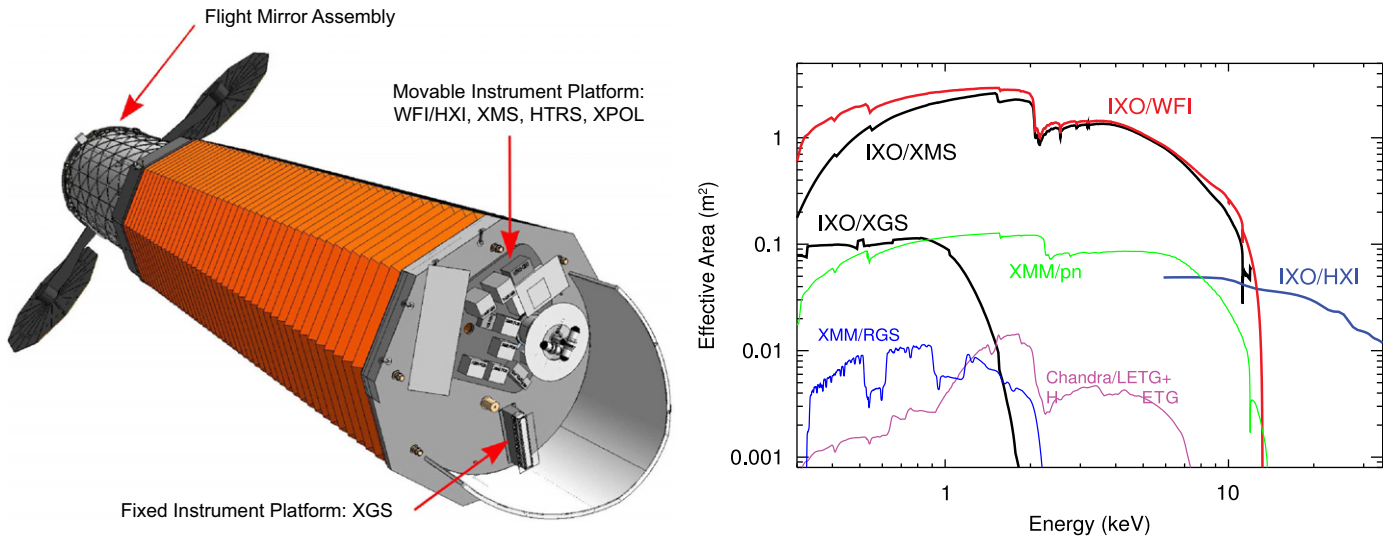
Fig. 1. Left: conceptual drawing of the IXO spacecraft and instrument platform (NASA study). To achieve the long focal length of 20 m in a way that is compatible with the launch vehicle fairing, the optical bench is mounted on an extensible instrument platform. The instrument platform consists of a Fixed Instrument Platform (FIP) on which the XGS is mounted as sole off-axis instrument, and a Moveable Instrument Platform (MIP), on which the complement of on-axis instruments (WFI/HXI, XMS, HTRS, XPOL) are mounted. The on-axis instruments are moved into focus individually as the science observations dictate. Right: effective area of various IXO instruments in comparison to XMM and Chandra heritage (NASA).

and *life cycles of matter and energy* (e.g. Refs. [7,8]). To address these questions, IXO's baseline instrumentation foresees suite of six instruments [9]:

WFI/ The *Wide-Field Imager* and *High-energy X-ray Imager* are HXI two independent instruments that are mounted behind each other in the same instrument slot of IXO's Movable Instrument Platform (MIP). As they share one position on the MIP, and thus always observe simultaneously, they can be considered as one instrument from the observatory standpoint. The WFI is an Active Pixel Sensor (APS) detector which covers a very large FoV of 18 ft × 18 ft with good spectral resolution ($\sim$ 125 eV at 5.9 keV), and good imaging resolution (fivefold oversampling of the mirror PSF) in the energy range of 0.1–15 keV. The HXI extends IXO's energy coverage to higher energies. It offers an 8 ft × 8 ft FoV with energy resolution of better than 1 keV (at 30 keV) in the energy band of 15–40 keV.

XMS The *X-ray Microcalorimeter Spectrometer* is a non-dispersive imaging high-resolution spectrometer, using an array of superconductive Transition Edge Sensors (TES). It has a spectral resolution of 2.5 eV in a field of view (FoV) of 2 ft × 2 ft, and 10 eV in an extended FoV of 5 ft × 5 ft.

HTRS The *High Time Resolution Spectrometer* is an array of 37 hexagonal Silicon Drift Diodes (SDD), placed out of focus so that the converging beam from the mirror assembly is distributed across the whole SDD array. This allows IXO to observe objects with fluxes of up to several tens of Crab without pile-up degradation with very high time resolution. The HTRS provides moderate (200 eV) energy resolution, but no imaging.

XPOL The *X-ray Polarimeter* is an imaging polarimeter, sensitive roughly to a 1% level polarisation of a 1 mCrab source in a 100 ks observation. It has a FoV of 2.6 ft × 2.6 ft, and a moderate energy resolution of $E/\Delta E \sim 5$ at 6 keV.

XGS The *X-ray Grating Spectrometer* is a non-imaging dispersive high resolution spectrograph. It is the only instrument that is operated constantly in parallel to the other instruments, as it diffracts light out of the main optical path onto its CCD detector array. The effective area used by the XGS is $A_{\text{eff}} = 1000\,\text{cm}^2$ (0.3–1.0 keV). It offers a very high spectral resolution of $\lambda/\Delta\lambda = 3000$.

The long focal length of the mirror system necessitates an extensible Deployment Module (DM). Retracted in its launch configuration, the DM allows IXO to fit into the fairing of either an Ariane 5 or an Atlas V launcher. Extended, it will move the instrument platform into position 20 m away from the mirror. Most of the instruments are on-axis instruments, therefore the optical bench will feature a Moveable Instrument Platform (MIP) that will move one on-axis instrument into focus at a time. The XGS is the only off-axis instrument and will therefore sit on the Fixed Instrument Platform (FIP) (see Fig. 1).

2. The IXO Wide Field Imager

One principal challenge encountered in the WFI is the need for very high readout rates. As can be seen in Fig. 1, the effective area of the IXO mirror system at 1 keV is more than a factor of 20 larger than previous X-ray missions, with correspondingly higher event rates. This necessitates very fast and flexible readout modes, in order to reduce event and pattern pile-up. Charge Coupled Device (CCD) sensors, which have been the predominant type of spectral imaging X-ray detector in recent decades, need to shift the signal charges across macroscopic distances, which inherently limits the speed with which signal charges can be accessed. Additionally, the Charge Transfer Efficiency (CTE), which is crucial for the performance of a CCD, depends on the quality of the bulk material and may deteriorate by radiation damage during the detector lifetime. This deterioration has for instance been observed in the Chandra ACIS and Suzaku XIS instruments [10].

For these reasons Active Pixel Sensors (APS), in which each pixel stores and amplifies the signal charge individually, have intrinsic advantages for the application in the IXO WFI. To achieve a field of view (FoV) of 18 ft, the WFI APS covers nearly the complete usable surface of a 6 in. wafer. Fig. 3 shows a mechanical prototype illustrating the physical and logical layout of the WFI APS.

As the WFI is fully depleted, signal charge generated by radiation entering from the backside of the detector can be detected efficiently. Backside illuminating the detector in this way allows the APS to have a geometrical fill factor of 100%. Furthermore, this allows us to use a very thin entrance window with consequently very good quantum efficiency in the energy regime below 1 keV. The large thickness of the fully depleted bulk provides for high quantum efficiency in the regime above 10 keV. However, as the large effective area X-ray mirror system does not only focus X-rays but also visible and UV light, care must be taken to avoid problematically high optical photon loads. Therefore, an optical blocking filter system consisting of a thin Al-layer on top of an UV blocking system is planned.

In order not to degrade the low-energy response in observations where it is critical for the science case, an option with a specific region on the APS left free from the optical/UV blocking filter is being evaluated. In this region, problems with a high optical load can be reduced e.g. by increased frame-rate if this region is defined as a region of interest and is read out preferentially (see Section 3 for details). Fig. 2 compares the expected performance of the WFI QE with the EPIC pn-CCD aboard XMM [11].

To achieve a roughly 5-times oversampling of the expected 5 in. (HEW) Point-Spread Function (PSF) of IXO's X-ray mirror system, the WFI baseline design foresees a pixel size of $100 \times 100\,\mu m^2$. Therefore, 1024×1024 pixels are needed to fully cover the 6 in. wafer. To facilitate monolithical integration, each corner of the detector has an area of the size of 128×128 pixels that is left free. As this area lies outside of the nominal FoV of the X-ray optics, it is shaded by the baffle system of the X-ray telescope, and the free corners do not limit the usable FoV (see Fig. 3).

To increase readout speed, the detector is subdivided into two hemispheres, each consisting of eight sectors read out by a dedicated readout ASIC. As the detector is backside illuminated and hemisphere division does not affect the pixels themselves but only the electrical interconnections between pixels, the geometrical fill-factor and quantum efficiency are not reduced by this division.
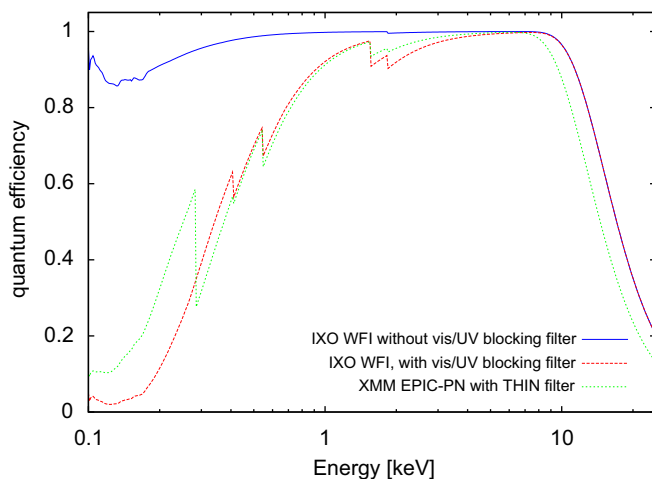
3. The DEPFET and its operation in WFI

The WFI APS is formed by a matrix of DEpleted P-channel Field-Effect Transistor (DEPFET) active pixels. While space-borne instruments using DEPFETs as detectors are only being implemented in the present day (e.g. Refs. [12,13]), the DEPFET principle is well described in the literature [14,15], so only a very brief introduction will be given here.

The DEPFET is a combined detector-amplifier structure that is formed by integrating a MOSFET onto a sideways-depleted silicon bulk (Fig. 4). With proper biasing and an additional deep-n implantation a potential minimum for electrons is formed underneath the MOSFET channel. Signal electrons trapped in this potential minimum influence the channel of the MOSFET similar to the gate, hence the potential minimum is named *internal gate*. A second FET-like structure called ClearFET is used to clear the signal charge from the internal gate in a controlled
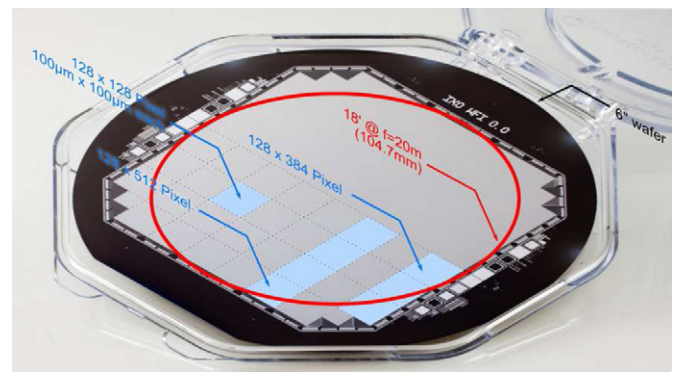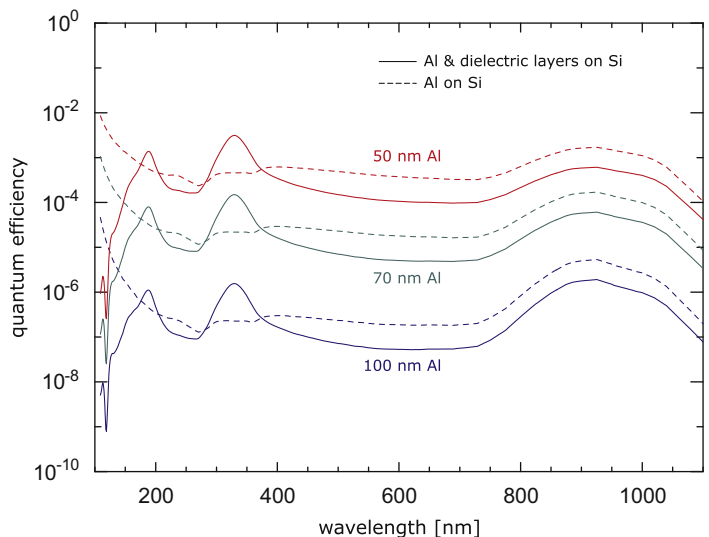

Fig. 3. Mechanical prototype of the IXO WFI wafer-scale detector. Overplotted on one hemisphere is the logical layout of the detector. The detector is monolithically integrated onto a 6-in. wafer. It consists of roughly 1024×1024 pixels of $100 \times 100\,\mu m^2$ size. The sensor is logically subdivided into two hemispheres, consisting of eight sectors each. Every sector is read out by a dedicated readout ASIC. To facilitate monolithical integration, the corners of the detector are left free. Shown here are two options: the overplotted graphics shows corners with 128×128 pixels per corner left free, the image shows a more complicated option.

Fig. 2. Expected WFI quantum efficiency curve (left) without and with UV/optical blocking filter (70 nm Al+SiO/SiN multilayer coating). Shown for comparison is the XMM quantum efficiency, using the thin optical blocking filter. The difference in the high energy regime is due to an increased bulk thickness in the WFI detector. The figure to the right shows the optical attenuation for various filter configurations.
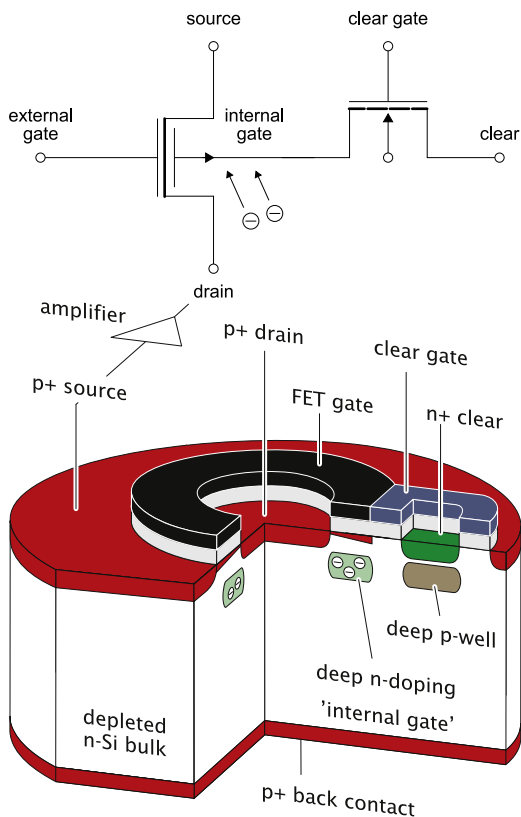
Fig. 4. Schematic representation and cutaway view of a circular MOS-type DEPFET pixel as implemented for the IXO WFI. The bulk thickness is 450 μm. The pixels consist of a circular p-channel MOSFET with an attached clear structure, formed by another MOS gate and an n$^+$-implantation. The clear structure forms an additional n-channel MOSFET, called ClearFET, contacting the internal gate.

manner, so a Correlated Double Sampling (CDS) readout scheme can be implemented: the amount of signal charge is derived from evaluation of the step in conductivity of the DEPFET before and after clearing the charge in the internal gate.

The conductivity of the channel can straightforwardly be sensed either in a source-follower configuration or by directly evaluating the drain current through the DEPFET. A source-follower configuration has the advantage that it can be AC-coupled to the readout amplifier, giving this solution an intrinsically very high robustness against transistor parameter variations and changes in operating conditions. The direct evaluation of the drain current on the other hand has the advantage of an increased speed: as all DEPFET terminal voltages are fixed, the source capacitance, which can be quite large in the case of long column lengths, does not have to be recharged.

Since the signal charge is both stored and read out in the DEPFET, each pixel of a two-dimensional matrix of pixels can in principle be read out individually. However, as pixel-individual connection would require a very high amount of routing resources and pixel-individual readout is not required in the scenario of the WFI, a simple interconnected matrix readout scheme is foreseen for the WFI.

In this readout scheme, all DEPFETs of the detector matrix share a common contact: either the drain contact in case of a source-follower configuration or the source-contact in the case of direct-current evaluation. Furthermore, the gate contacts within each row and the source (source-follower) or drain (direct current) contacts within each column are interconnected. If exactly one DEPFET per column is turned on, the current through the column is the current through that DEPFET. This allows addressing a specific pixel by

turning on the DEPFETs in the corresponding row, and sensing the current through the respective column. Fig. 5 gives an overview of the matrix interconnection, using a source-follower configuration as example.

Since the DEPFET pixels are read out by sensing the conductivity change of the DEPFET created by the signal charge collected in the internal gate, the contacts controlling the ClearFET are also interconnected row-wise. In effect, a row-wise "rolling shutter" type readout is implemented by turning on all DEPFETs in one row, and sensing the current through the DEPFETs column-wise. In a second step, a clear voltage is applied to all pixels in one row, and the clear gate of all pixels of this row is opened for long enough to completely remove the signal charge through the clear contact of the row. After closing the clear gate the current through the now empty DEPFETs is sensed again.

After the readout cycle of a row is finished, the current through the row's DEPFETs is turned off, and the next row is turned on and read out. Thus, the complete matrix is read out row by row. After all rows of the matrix have been read out, the readout cycle starts anew from the first row. As each row stays sensitive during the readout of all other rows using this kind of rolling shutter readout, the integration time of each row is the sum of the readout times of all rows.

In order to avoid pile-up at high photon-rates, it is desirable to decrease the overall exposure time of each pixel, effectively increasing the frame-rate. The most obvious way to increase the frame-rate is to read out more than one row at a time. In the WFI, this is implemented in a straightforward way by bisecting column-wise source-interconnects in the center of the APS, and reading out one full row in each hemisphere simultaneously. For a row processing time of 2−4 μs, a full-frame rate of 500–1000 fps can be achieved in this way.

Additionally, the matrix interconnect allows a number of flexible readout modes. Since the signal charge in one DEPFET is not modified by another DEPFET's operation, a small region of interest (RoI) can be defined in the rows surrounding a bright source. If the RoI has only a fraction of the rows of the full hemisphere, the repetition rate is very high when only the RoI is repeatedly read out. The charge in the rest of the frame can be read out at a lower rate by performing a full-frame readout every n RoI readouts.

Given a reasonably flexible control electronics, a number of variations on this RoI readout scheme are possible [9].

4. Front-end electronics

As seen above, pixels are controlled by toggling a sequence of voltages on the gate, clear gate and clear contacts of each row, and sensing the current through each column. The correct sequence of voltages of each row is applied by the SWITCHER ASIC [16], a 64 channel, dual output, high voltage switching circuit manufactured in an AMS 0.8 μm high voltage CMOS process. It has been designed specifically for the purpose of DEPFET matrix readout and provides two output ports for every channel, which can be toggled between two individual voltages each. Facilities for precise timing of the switching process and easy integration of a large number of SWITCHER ICs make it a suitable device for building a daisy chain to read out large sensor arrays. The total switch voltage difference can be as large as 20 V. Based on this heritage, a radiation hard variant of the IC using the 0.35 μm AMS 3.3 V CMOS process using the high voltage option is under development.

The current through the DEPFET is sensed by a multi-channel signal shaper/amplifier ASIC. Each column of the sensor array is read out individually by one channel of an Analog Front-End (AFE)
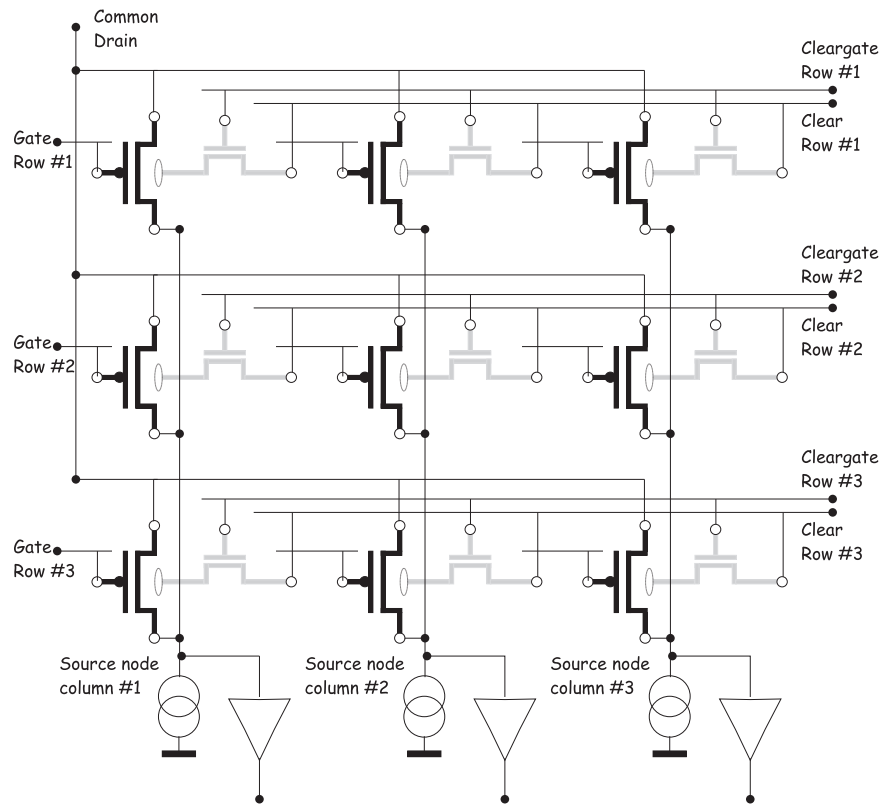
Fig. 5. Matrix interconnection scheme as used in WFI. Shown here as representative example is the source-follower configuration. Using a row-wise rolling shutter readout, gate, cleargate and clear contacts of all pixels in one row are interconnected. In the source-follower case the drain contact of all pixels is shared globally, while all source contacts in one column are interconnected. In the drain based current readout scheme, the drain and source roles are interchanged, resulting in an inversion of pixel topology.
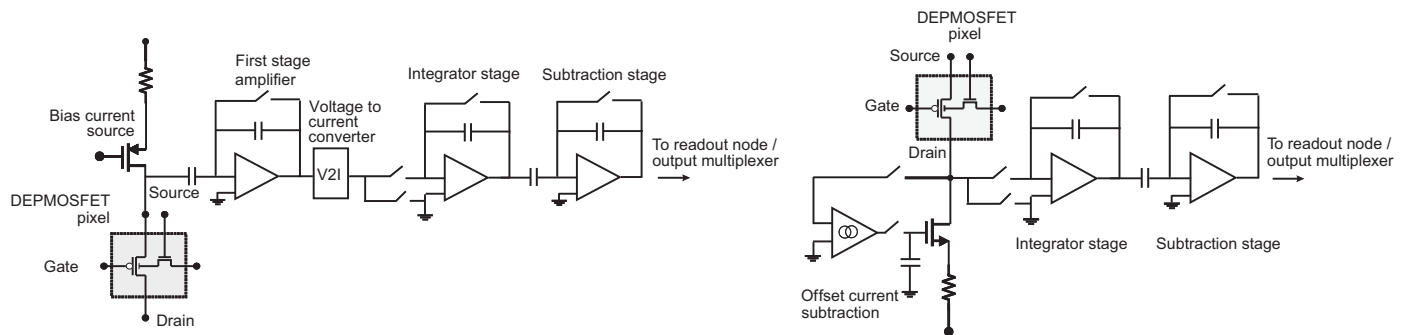

Fig. 6. Block diagrams of one channel of the two options under study for the IXO analog front end ASICs. The ASTEROID (left) implements a source-follower readout with an AC-coupled first stage amplifier, which interfaces to the integrator stage by a voltage-to-current converter. The VELA (right) implements the drain-based current readout scheme and has a low-noise bias current subtraction stage at the input. Both devices implement trapezoidal filtering with a combination of integration and subtraction stages.

ASIC. This ASIC not only filters and amplifies the signal, but also intrinsically subtracts the empty-pixel baseline from the signal, and serializes the column-parallel readout to a stream of analog voltages. The baseline for WFI assumes 128 channel AFE ASICs with two serial output channels each. Therefore there are going to be a total of 16 AFE ASICs and 32 serial analog outputs to digitize and further process.

Two different AFE solutions implementing trapezoidal filtering have been designed, and 64 channel ASIC prototypes have been developed. Trapezoidal filtering is optimal in case white series noise is the dominant noise source [17], which is the case for the DEPFET device in the IXO readout speed regime of $2-4\,\mu s$ per row.

Both AFE ASIC developments implement shaping by means of current integration and subtraction stages. One of the designs, the VLSI ELectronics for Astronomy (VELA) IC [18] is designed for drain-based current readout and directly integrates the current provided by the pixel device; to use the amplifier's dynamic range more efficiently, the offset current of the pixel is subtracted prior to signal acquisition. The other design, called ASTEROID (Active current Switching TEchnique ReadOut In X-ray spectroscopy with DEPFET) [19], implements the source follower readout scheme using the same shaper, but a combination of a first stage amplifier and a voltage-to-current converter for interfacing source follower and shaper. Block diagrams of the two structures are shown in Fig. 6. In spite of their different input stages, both ICs have

identical filtering stages, followed by a sample & hold circuit and a sequencer-controlled analog output multiplexer.

To control the filter and multiplexer timing, the filter sequence is stored within an on-chip sequencer RAM. The ICs also offer on-chip DACs for setting the bias points of the various amplifier stages, a very fast and flexible, sequencer controlled analog output multiplexer, the possibility to inject arbitrary test patterns and a system-friendly SPI control interface. The on-chip memory was implemented using Dual Port DICE (Dual Interlocked Storage Cells) to increase robustness against Single Event Upset (SEU) events. Sixty-four channel versions of both ICs have been developed and are being examined with respect to their suitability for the IXO WFI instrument. Both ICs have been made in an $0.35\,\mu m$ AMS 3.3 V CMOS process, and have already proven their suitability for the use with DEPFET devices (see Section 5).

Baseline for IXO is the VELA IC, because of the advantages in speed of the drain based current readout. Nevertheless, an ASTEROID based source-follower readout is still pursued as backup option, as the AC-coupled source-follower offers intrinsic advantages e.g. with respect to robustness against pixel-to-pixel variations across the matrix, or parameter shifts due to radiation damage. It is expected that row speeds of $\sim 2\,\mu s$ can be reached using VELA, and $\sim 3.5\,\mu s$ using ASTEROID.

5. Prototype device status

Since the beginnings of DEPFET development, a large variety of DEPFET matrix devices, from single pixels and small 64×64, $75 \times 75\,\mu m^2$ devices [20] up to large DEPFET Macropixel devices consisting of 64×64 pixels of $0.5 \times 0.5\,mm^2$ size and having an overall sensitive area of $3.2 \times 3.2\,cm^2$, have been built and tested at the MPI semiconductor lab. The production yield was generally very good, as shown, e.g., on large Macropixel devices [13], where the yield was found to be above 70%. Cosmetic defects, e.g. bright or noisy pixels, were very rare, making most good devices perfect. The devices show near Fano-limited energy resolution even at fast readout speeds (see Fig. 7).
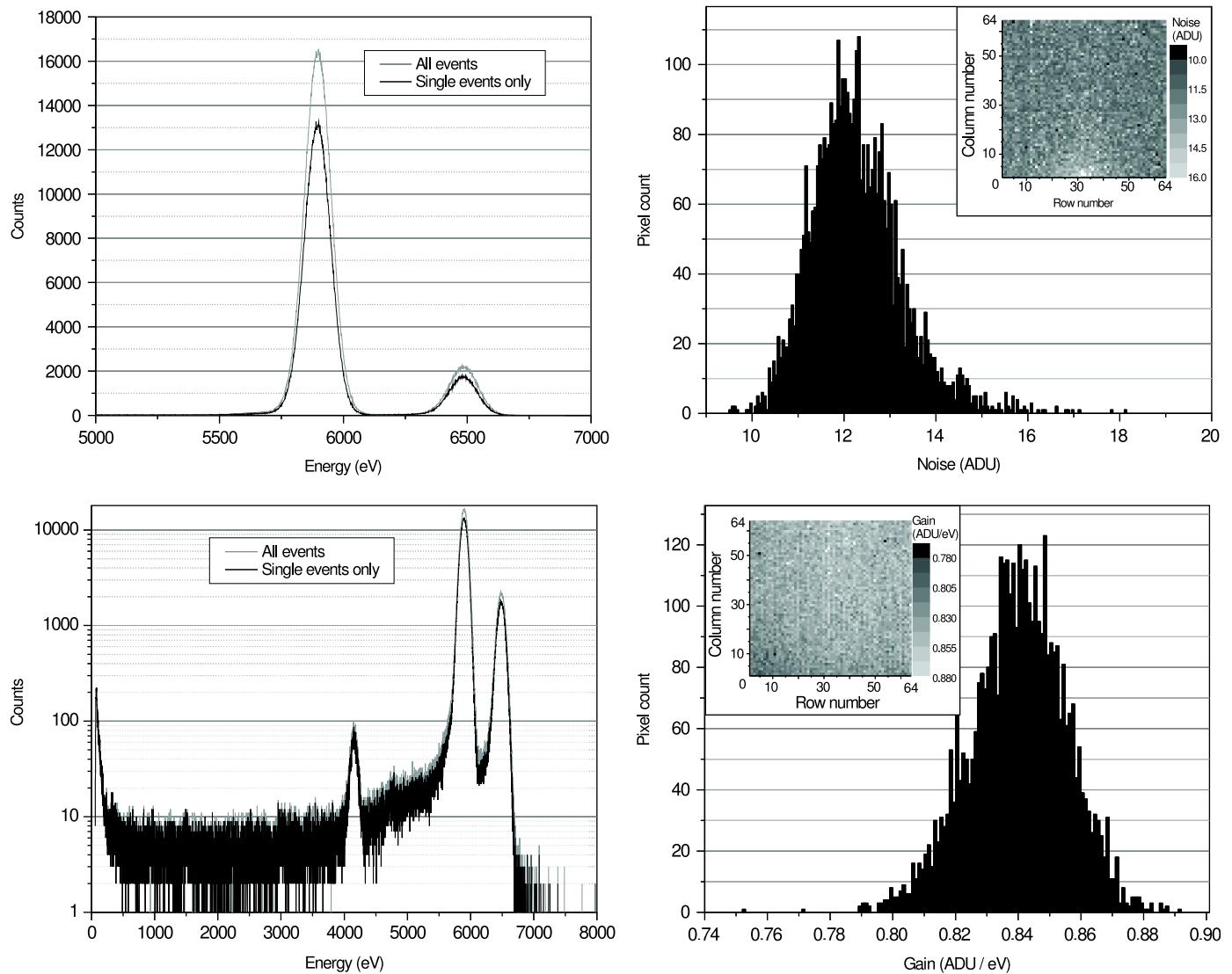

Fig. 7. In the left column, typical ^{55}Fe spectra as measured with a Macropixel device and an ASTEROID readout ASIC are shown. Processing time was 6.2 μs per row. Selecting only single pixel events, the measured energy resolution is 126 eV FWHM at 5.9 keV, integrating all valid pattern events it is 128 eV FWHM at 5.9 keV. The logarithmically plotted spectrum in the lower graph shows a peak-to-background ratio of ~ 3000, qualifying the device as spectroscopy-grade X-ray detectors. In the right column, a typical noise-map (upper graph) and gain-map (lower graph) are shown. Neither dead nor noisy pixels are apparent. The gain dispersion is $\sim 2.5\%$, the noise dispersion is $\sim 8\%$. The noise dispersion in this setup is affected by insufficiently shielded IR radiation from the nearby ASTEROID ASIC.

Current work towards WFI large area detectors is the operation of 256×256, pixel matrices with $75 \times 75\,\mu m^2$ pixels. The operation of these prototypes has recently been started. They are read out by four readout ASICs running in parallel, for the first time showing the multiple ASIC operation envisaged for each WFI detector hemisphere.

The next step of prototype development is the production and operation of WFI quadrant prototypes. These devices, 512×512, pixel matrices with $100 \times 100\,\mu m^2$ pixels, are identical to the full WFI detector in many important aspects like pixel size column and length. The properties of these devices therefore will allow estimate the properties of the wafer-scale WFI detector with high confidence. This will allow to decide between the direct drain current readout (VELA) and the source follower configuration (ASTEROID). Furthermore, the large area of $5.12 \times 5.12\,cm^2$ and high pixel count will allow yield estimates with high confidence for the wafer-scale WFI devices.

6. Summary and outlook

The planned Wide-Field Imager (WFI) of the International X-ray Observatory (IXO) is based on an Active Pixel Sensor (APS) built using DEPFET pixel elements. Its monolithical implementation on a 6 in. wafer gives the WFI the maximum unobstructed field of view available. The DEPFET technology employed enables the WFI to provide very high energy resolution while reading out at very high frame-rates. As the integrated signal of one pixel is not influenced by another pixel's readout, even higher frame-rates are possible for reduced area regions of interest with very flexible readout modes. The high data-rate generated by the APS requires fast, low-noise Analog Front End electronics and sophisticated on-board data reduction, which are currently under development. Tests using existing DEPFET matrices and Analog Front End Prototypes have shown very promising results. Tests of larger physical and logical area prototypes and production of very large WFI quadrant prototypes are under way.

References

[1] K. Nandra, Astronomy 2010 (2009) 220 arXiv:0903.0547.
[2] L. Brenneman, J. Miller, P. Nantra, M. Volonteri, M. Cappi, G. Matt, S. Kitamoto, F. Paerels, M. Mendez, R. Smith, M. Nowak, M. Garcia, M. Watson, M. Weisskopf, Y. Terashima, Y. Ueda, Astronomy 2010 (2009) 26 arXiv:0902.4691.
[3] F. Paerels, M. Méndez, M. Agueros, M. Baring, D. Barret, S. Bhattacharyya, E. Cackett, J. Cottam, M. Diaz Trigo, D. Fox, M. Garcia, E. Gotthelf, W. Hermsen, W. Ho, K. Hurley, P. Konker, A. Juett, P. Kaaret, O. Kargaltsev, J. Lattimer, G. Matt, F. Özel, G. Pavlov, R. Rutledge, R. Smith, L. Stella, T. Strohmayer, H. Tananbaum, P. Uttley, M. van Kerkwijk, M. Weisskopf, S. Zane, Astronomy 2010 (2009) 230 arXiv:0904.0435.
[4] A. Vikhlinin, S.W. Allen, M. Arnaud, M. Bautz, H. Böhringer, M. Bonamente, J. Burns, A. Evrard, J.P. Henry, C. Jones, B.R. McNamara, D. Nagai, D. Rapetti, T. Reiprich, Astronomy 2010 (2009) 304 arXiv:0903.2297.
[5] A.C. Fabian, E. Churazov, M. Donahue, W.R. Forman, M.R. Garcia, S. Heinz, B.R. McNamara, K. Nandra, P. Nulsen, P. Ogle, E.S. Perlman, D. Proga, M.J. Rees, C.L. Sarazin, R.A. Sunyaev, G.B. Taylor, S.D.M. White, A. Vikhlinin, D.M. Worrall, Astronomy 2010 (2009) 73 arXiv:0903.4424.
[6] J.N. Bregman, R.A. Benjamin, M. Bonamente, C.R. Canizares, A. Hornschemeier, E. Jenkins, F.J. Lockman, F. Nicastro, T. Ohashi, F. Paerels, M.E. Putman, K. Sembach, N. Schulz, B. Savage, R. Smith, N. Yamasaki, Y. Yao, B. Wakker, Astronomy 2010 (2009) 25 arXiv:0906.4993.
[7] J.P. Hughes, C. Badenes, A. Bamba, W. Blair, A. Decourchelle, D. Dewey, C. Fryer, U. Hwang, J.M. Laming, K. Nomoto, S. Park, D. Patnaude, P. Plucinsky, L. Rudnick, P. Slane, F.-K. Thielemann, J. Vink, P.F. Winkler, Astronomy 2010 (2009) 136.
[8] D.K. Strickland, A. Hornschemeier, A. Ptak, E. Schlegel, C. Tremonti, T. Tsuru, R. Tüllmann, A. Zezas, Astronomy 2010 (2009) 289 arXiv:0902.2945.
[9] IXO Payload Definition Document, Technical Note SRE-PA/2009.019, ESA, April 2009. URL: ⟨http://sci.esa.int/science-e/www/object/index.cfm?fobjectid=44697⟩.
[10] B. LaMarr, C. Grant, S. Kissel, G. Prigozhin, M. Bautz, T.G. Tsuru, H. Tsunemi, T. Dotani, K. Hayashida, H. Matsumoto, Front- and back-illuminated X-ray CCD performance in low- and high-Earth orbit: performance trends of Suzaku XIS and Chandra ACIS detectors, in: Society of Photo-Optical Instrumentation Engineers (SPIE) Conference Series, Society of Photo-Optical Instrumentation Engineers (SPIE) Conference Series, vol. 7011, 2008. doi: 10.1117/12.788168.
[11] L. Strüder, U. Briel, K. Dennerl, et al., Astron. Astrophys. 365 (1) (2001) L18.
[12] J. Treis, et al., Nucl. Instr. and Meth. A 568 (2006) 191.
[13] J. Treis, et al., DEPFET based X-ray detectors for the MIXS focal plane on BepiColombo, in: A.D. Holland, D.A. Dorn (Eds.), High Energy, Optical, and Infrared Detectors for Astronomy III, SPIE Proceedings, vol. 7021, 2008, p. 70210Z-1.
[14] J. Kemmer, G. Lutz, Nucl. Instr. and Meth. A 253 (1987) 356.
[15] J. Kemmer, et al., Nucl. Instr. and Meth. A 288 (1990) 92.
[16] J. Treis, et al., First results of DEPFET based Active Pixel Sensor prototypes for the XEUS Wide Field Imager, in: A.D. Holland (Ed.), High-Energy Detectors in Astronomy, SPIE Proceedings, vol. 5501, 2004, p. 89.
[17] M. Porro, et al., Nucl. Instr. and Meth. A 512 (2003) 179.
[18] L. Bombelli, et al., Fast DEPFET read-out for the Simbol-X low energy detector, in: IEEE NSS Conference Record 2008 IEEE Nuclear Science Symposium Conference Record, 2008, pp. N21–N23.
[19] M. Porro, et al., Performance of ASTEROID: a 64 channel ASIC for source follower readout of depfet matrices for X-ray astronomy, in: IEEE NSS Conference Record 2008 IEEE Nuclear Science Symposium Conference Record, 2008, pp. N23–N26.
[20] J. Treis, et al., IEEE Trans. Nucl. Sci. NS-52 (2005) 1083.